

This is the accepted manuscript made available via CHORUS. The article has been published as:

Theoretical study of the $\alpha+d\rightarrow^6\text{Li}+\gamma$ astrophysical capture process in a three-body model. II. Reaction rates and primordial abundance

E. M. Tursunov, S. A. Turakulov, A. S. Kadyrov, and I. Bray

Phys. Rev. C **98**, 055803 — Published 21 November 2018

DOI: [10.1103/PhysRevC.98.055803](https://doi.org/10.1103/PhysRevC.98.055803)

Theoretical study of the direct $\alpha + d \rightarrow {}^6\text{Li} + \gamma$ astrophysical capture process in a three-body model II. Reaction rates and primordial abundance

E. M. Tursunov,^{1,2,*} S. A. Turakulov,^{1,†} A. S. Kadyrov,^{2,‡} and I. Bray^{2,§}

¹*Institute of Nuclear Physics, Academy of Sciences, 100214, Ulugbek, Tashkent, Uzbekistan*

²*Curtin Institute for Computation and Department of Physics and Astronomy,
Curtin University, GPO Box U1987, Perth, WA 6845, Australia*

The astrophysical S-factor and reaction rate of the direct capture process $\alpha + d \rightarrow {}^6\text{Li} + \gamma$, as well as the abundance of the ${}^6\text{Li}$ element are estimated in a three-body model. The initial state is factorized into the deuteron bound state and the $\alpha + d$ scattering state. The final nucleus ${}^6\text{Li}(1+)$ is described as a three-body bound state $\alpha + n + p$ in the hyperspherical Lagrange-mesh method. Corrections to the asymptotics of the overlap integral in the S- and D-waves have been done for the E2 S-factor. The isospin forbidden E1 S-factor is calculated from the initial isosinglet states to the small isotriplet components of the final ${}^6\text{Li}(1+)$ bound state. It is shown that the three-body model is able to reproduce the newest experimental data of the LUNA collaboration for the astrophysical S-factor and the reaction rates within the experimental error bars. The estimated ${}^6\text{Li}/\text{H}$ abundance ratio of $(0.67 \pm 0.01) \times 10^{-14}$ is in a very good agreement with the recent measurement $(0.80 \pm 0.18) \times 10^{-14}$ of the LUNA collaboration.

PACS numbers: 11.10.Ef, 12.39.Fe, 12.39.Ki

I. INTRODUCTION

There are two open astrophysical problems related to the abundance of lithium elements in the Universe. First, the Big Bang nucleosynthesis (BBN) model predicts for the ${}^7\text{Li}/\text{H}$ ratio an estimate about three times larger than the recent astronomical observational data from metal-poor halo stars [1, 2]. The second lithium puzzle is related to the estimation of the primordial abundance ratio ${}^6\text{Li}/{}^7\text{Li}$ of the lithium isotopes. For this ratio the BBN model [3] yields a value about three orders of magnitude less than the astrophysical data [4]. In the BBN model the abundance of the ${}^7\text{Li}$ element is estimated on the basis of two key capture reactions $\alpha({}^3\text{He}, \gamma){}^7\text{Be}$ and $\alpha({}^3\text{H}, \gamma){}^7\text{Li}$ (see [5–7] and references therein). For the estimation of the ${}^6\text{Li}/{}^7\text{Li}$ ratio the BBN model includes as input parameters the reaction rates of the direct radiative capture process



at low energies within the range $30 \leq E_{\text{cm}} \leq 400$ keV [3]. The data set of the LUNA collaboration at two astrophysical energies $E=94$ keV and $E=134$ keV [8] was recently renewed with additional data at $E=80$ keV and $E=120$ keV [9]. These data sets were obtained as results of the direct measurements of the astrophysical S-factor at the underground facility. The new data are lower than the old data of nondirect measurements from Ref. [10]. Based on the new data set, the thermonuclear reaction rate of the process has been estimated by the LUNA collaboration. The results for the reaction rates turn out

to be even lower than previously reported. This further increases the discrepancy between prediction of the BBN model and the astronomical observations for the primordial abundance of the ${}^6\text{Li}$ element in the Universe [9].

Until recently all the theoretical estimations of the astrophysical S-factor of the above direct capture reaction at low astrophysical energies were based on the so-called exact mass prescription, in the both potential models [2, 11–15] and microscopic approaches [16, 17]. The microscopic models [18, 19] deal with only E2 transition operator, neglecting a contribution of the E1-transition operator to the astrophysical S-factor. Within this prescription the matrix elements of the isospin forbidden E1-transition were estimated by using the exact experimental mass values of the colliding nuclei ${}^2\text{H}$ and ${}^4\text{He}$. As was shown recently in Ref. [20] in details, this way has no microscopic background at all and cannot be used, for example in the description of the capture process $d(d, \gamma){}^4\text{He}$ of two identical nuclei. Of course, the estimated in this way cross sections and S-factors of the $\alpha(d, \gamma){}^6\text{Li}$ capture reaction can be fortuitously close to the experimental data, however this method does not yield a relevant energy dependence of the S-factor and cross section and correct predictive power for future *ab-initio* studies [20]. An alternative approach to the description of the capture processes is based on solving the three-body Faddeev equations [21] using quasi-separable potentials. An advantage of this method is that it allows an easier treatment of non-local effects that can be extended to three-body problems.

Realistic three-body models are based on the isovector E1 transition from the initial $T_i = 0$ (isosinglet) states to the $T_f = 1$ (isotriplet) components of the final ${}^6\text{Li}(1+)$ bound state, or from the initial isotriplet components to the main isoscalar part of the final ${}^6\text{Li}(1+)$ nucleus bound state [20]. First attempt to estimate in a correct way the matrix elements of the isospin-forbidden E1- transition

* tursune@inp.uz

† turakulov@inp.uz

‡ a.kadyrov@curtin.edu.au

§ i.bray@curtin.edu.au

together with the E2-transition for the ${}^4\text{He}(d, \gamma){}^6\text{Li}$ direct capture process has been done in the three-body model [22]. The formalism of the model has been developed in a consistent way and correct analytical expressions have been obtained for the matrix elements of the E1- and E2-transitions, including the isovector transition matrix elements. The numerical results were obtained on the basis of the final three-body wave function ${}^6\text{Li} = \alpha + p + n$ in hyperspherical coordinates [23, 24], which had a small isotriplet component with the norm square of 1.13×10^{-5} . Due to smallness of the isotriplet component of the final three-body bound state the corresponding numerical calculations in Ref. [22] have reproduced the existing experimental data for the S-factor only in the frame of the exact mass prescription and with the help of additional spectroscopic factor. Further studies in Ref. [20] have demonstrated that the quality of the final three-body wave function ${}^6\text{Li} = \alpha + p + n$ can be improved and convergent isotriplet component can be reached with the norm square of 5.3×10^{-3} , which is larger than the old number by two orders of magnitude. This led to the fact that the E1 S-factor also increased by two orders of magnitude. Additionally, as was shown in that paper, the E2 S-factor can be improved owing to the correction of the S-wave asymptotics of the overlap integral of the ${}^6\text{Li}$ and deuteron wave functions at a distance 5-10 fm. Below we describe an influence of the correction to the D-wave asymptotics of the overlap integral on the E2 S-factor and the reaction rates at low energies.

The aim of present study is to estimate the reaction rates of the $\alpha(d, \gamma){}^6\text{Li}$ direct capture process and the primordial abundance of the ${}^6\text{Li}$ element in the Universe within the improved realistic three-body model [20, 22]. The initial wave function is factorized into the deuteron bound-state and the α - d scattering-state wave functions. The final ${}^6\text{Li}(1+)$ state is described as a $\alpha + p + n$ three-body bound system. The wave function on the hyperspherical Lagrange mesh basis available for the ${}^6\text{Li}(1+)$ bound state [23, 24] will be employed.

The hyperspherical harmonics method is an effective tool, widely used in the literature for the description of the three-body bound states of halo nuclei [25], resonances and non-resonant continuum [26, 27]. The Faddeev hyperspherical harmonics method was applied to the three-body problem with a core excitation [28], while its combination with the R-matrix approach has been applied to estimate the triple α rate in a full three-body model [29]. The harmonic oscillator basis method have been applied to the description of the bound and continuum spectrum of the halo nucleus ${}^6\text{He}$ [30], and three-body capture [31] of this nucleus. The hyperspherical R-matrix method was also applied to the description of two-neutron emission of the ${}^{16}\text{Be}$ halo nucleus [32], and $\alpha + \alpha + n + {}^{208}\text{Pb}$ four-body scattering, breakup and fusion processes [33] as an alternative to complex range Gaussian basis [34] method. As an astrophysical application, in Ref. [35] the hyperspherical adiabatic expansion method was used for the estimation of relative produc-

tion rates and abundance of the ${}^6\text{He}$, ${}^9\text{Be}$ and ${}^{12}\text{C}$ nuclei in a three-body model.

In Sec. II we describe the model, in Sec. III we discuss obtained numerical results and finally, in the last section we draw conclusions.

II. THEORETICAL MODEL

A. Cross sections of the radiation capture process

The cross sections of the radiative capture process reads

$$\sigma_E(\lambda) = \sum_{J_i T_i \pi_i} \sum_{J_f T_f \pi_f} \sum_{\Omega \lambda} \frac{(2J_f + 1)}{[I_1][I_2]} \frac{32\pi^2(\lambda + 1)}{\hbar \lambda ([\lambda]!!)^2} k_\gamma^{2\lambda+1} C_s^2 \times \sum_{l_\omega I_\omega} \frac{1}{k_\omega^2 v_\omega} |\langle \Psi^{J_f T_f \pi_f} \| M_\lambda^\Omega \| \Psi_{l_\omega I_\omega}^{J_i T_i \pi_i} \rangle|^2, \quad (2)$$

where $\Omega = \text{E or M}$ (electric or magnetic transition), ω denotes the entrance channel, k_ω , v_ω , I_ω are the wave number, velocity of the $\alpha - d$ relative motion and the spin of the entrance channel, respectively, J_f , T_f , π_f (J_i , T_i , π_i) are the spin, isospin and parity of the final (initial) state, I_1 , I_2 are channel spins, $k_\gamma = E_\gamma/\hbar c$ is the wave number of the photon corresponding to the energy $E_\gamma = E_{\text{th}} + E$ with the threshold energy $E_{\text{th}} = 1.474$ MeV. The wave functions $\Psi_{l_\omega I_\omega}^{J_i T_i \pi_i}$ and $\Psi^{J_f T_f \pi_f}$ represent the initial and final states, respectively. The reduced matrix elements are evaluated between the initial and final states. We also use short-hand notations $[I] = 2I + 1$ and $[\lambda]!! = (2\lambda + 1)!!$.

Constant C_s^2 is the spectroscopic factor [36]. As argued in Ref. [14], if the two-body potentials of the model correctly reproduce experimental phase shifts in the partial waves and physical bound state energies of the two-body subsystems, then a value of the spectroscopic factor must be taken equal to 1. This reflects the fact that the potential parameters already include many-body effects. Accordingly, the factor is set equal to 1.

The analytical expressions of the E1 and E2 electric-transition operators, including isospin transition operators and their matrix elements in the three-body model have been described in Ref. [22]. For the sake of brevity we refer to that paper for the details of the model.

The astrophysical S -factor of the process is expressed in terms of the cross section as [37]

$$S(E) = E \sigma_E(\lambda) \exp(2\pi\eta), \quad (3)$$

where η is the Coulomb parameter.

B. Reaction rates

The reaction rate $N_a(\sigma v)$ is estimated according to [36, 37]

$$N_A(\sigma v) = N_A \frac{(8/\pi)^{1/2}}{\mu^{1/2} (k_B T)^{3/2}} \int_0^\infty \sigma(E) E \exp(-E/k_B T) dE, \quad (4)$$

where k_B is the Boltzmann constant, T is the temperature, $N_A = 6.0221 \times 10^{23} \text{ mol}^{-1}$ is the Avogadro number. The reduced mass is written as $\mu = A m_N$ with the corresponding reduced mass number $A = A_1 A_2 / (A_1 + A_2)$ for the $\alpha + d$ system, where $A_1 = 2$ and $A_2 = 4$. Consequently, a value of $A = 4/3$ is fixed. When a variable $k_B T$ is expressed in units of MeV it is convenient to use a variable T_9 for the temperature in units of 10^9 K according to the equation $k_B T = T_9 / 11.605$ MeV. In our calculations T_9 varies in the interval $0.001 \leq T_9 \leq 10$.

After substitution of these variables the above integral for the reaction rates can be expressed as:

$$N_A(\sigma v) = 3.7313 \times 10^{10} A^{-1/2} T_9^{-3/2} \times \int_0^\infty \sigma(E) E \exp(-11.605 E / T_9) dE. \quad (5)$$

III. NUMERICAL RESULTS

A. Details of the calculations

Calculations of the cross section and astrophysical S-factor have been performed under the same conditions as in Ref.[20]. The radial wave function of the deuteron is the solution of the bound-state Schrödinger equation with the central Minnesota potential V_{NN} [38, 39] with $\hbar^2/2m_N = 20.7343$ MeV fm². The Schrödinger equation is solved using a highly accurate Lagrange-Laguerre mesh method [40]. It yields $E_d = -2.202$ MeV for the deuteron ground-state energy with the number of mesh points $N = 40$ and a scaling parameter $h_d = 0.40$.

The scattering wave function of the $\alpha - d$ relative motion is calculated with a deep potential of Dubovichenko [41] with a small modification in the S -wave [15]: $V_d^{(S)}(R) = -92.44 \exp(-0.25 R^2)$ MeV. The potential parameters in the 3P_0 , 3P_1 , 3P_2 and 3D_1 , 3D_2 , 3D_3 partial waves are the same as in Ref. [41]. The potential contains additional states in the S - and P -waves forbidden by the Pauli principle. The above modification of the S -wave potential reproduces the empirical value $C_{\alpha d} = 2.31 \text{ fm}^{-1/2}$ of the asymptotic normalization coefficient (ANC) of the $^6\text{Li}(1+)$ ground state derived from $\alpha - d$ elastic scattering data [42].

The final $^6\text{Li}(1+)$ ground-state wave function was calculated using the hyperspherical Lagrange-mesh method [23, 24, 43] with the same Minnesota NN-potential. For the $\alpha - N$ nuclear interaction the potentials of Voronchev *et al.* (Model A) [44] and Kanada *et al.* (Model B)

[45] were employed, which contain a deep Pauli-forbidden state in the S -wave. The potentials were slightly renormalized by a scaling factors 1.014 (Model A) and 1.008 (Model B) to reproduce the experimental binding energy $E_b = 3.70$ MeV. The Coulomb interaction between α and proton is taken as $2e^2 \text{erf}(0.83 R)/R$ [39]. The coupled hyperradial equations are solved with the Lagrange-mesh method [23, 40]. The hypermomentum expansion includes terms up to a large value of K_{max} , which ensures a good convergence of the energy and of the $T = 1$ component of ^6Li . For the treatment of Pauli forbidden states in the three-body system we employ a method of orthogonalizing pseudopotentials (OPP) [46] as an alternative to the method of supersymmetric transformation (SUSY) [47].

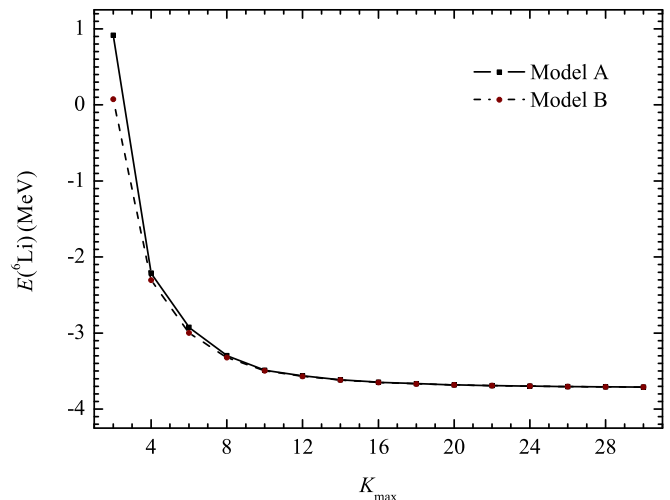


FIG. 1. Convergence of the ^6Li ground state energy with respect to K_{max} within Models A and B

In Fig. 1 we display the convergence of the ^6Li ground state energy with respect to the maximal hypermomentum K_{max} . In particular, for $K_{\text{max}} = 20$ the level of convergence is better than 1% within Model A which is based on the $\alpha - N$ potential of Voronchev *et al.* [44]. In the case of $K_{\text{max}} = 24$, the level of convergence is better than 0.2%, while for the $K_{\text{max}} = 30$, it is 0.1%. The same convergence behavior is observed within Model B with the $\alpha - N$ potential of Kanada *et al.*. One can conclude that the energy of the three-body system is well converged already at $K_{\text{max}} = 20$. At the same time, the norm square of the $T=1$ isotriplet components of the three-body wave function, which is important for the isospin forbidden E1-transition, is within $(5.3-5.4) \times 10^{-3}$ and $(4.2-4.3) \times 10^{-3}$ in Models A and B, respectively, for the values of $K_{\text{max}} = 12-30$. For the case of $K_{\text{max}} = 24$ the ground state is essentially spin triplet (96 %). The matter r.m.s. radius of the ground state (with 1.4 fm as α radius) is found as $\sqrt{r^2} \approx 2.25$ fm with the potential of Ref. [44] or 2.24 fm with the potential of Ref. [45], *i.e.* values slightly lower than the experimental value 2.32 ± 0.03 fm [48]. The isotriplet component in the ^6Li ground state has a

squared norm 5.3×10^{-3} with the potential of Ref. [44] (Model A) and 4.2×10^{-3} with the potential of Ref. [45] (Model B).

B. Estimation of the astrophysical S-factor

In Fig. 2 we display E1 astrophysical S-factors for the direct $\alpha + d \rightarrow {}^6\text{Li} + \gamma$ capture process within Model A from the initial partial 3P_0 , 3P_1 , 3P_2 scattering waves to the $T=1$ (isotriplet) components of the final ground state of ${}^6\text{Li}$.

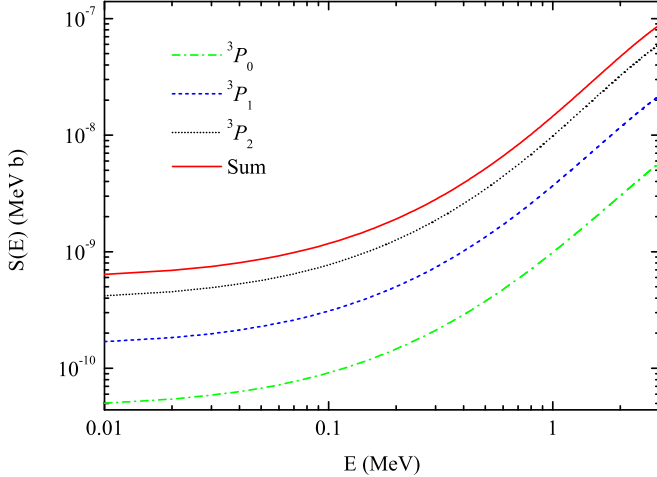


FIG. 2. Partial E1 astrophysical S-factors of the direct $\alpha + d \rightarrow {}^6\text{Li} + \gamma$ capture process within Model A (see text).

At low astrophysical energies, the E2 cross section is very sensitive to the asymptotic behavior of the overlap integrals of the deuteron wave function Ψ_d and the three-body wave functions Ψ_f^{1M+} for the $L=0$ and $L=2$ partial waves up to large $\alpha-d$ distances R . The asymptotic normalization coefficients (ANCs) of the ${}^6\text{Li}$ nucleus in the $\alpha + d$ channel can be extracted within the effective range expansion method [49, 50] or from the analytical continuation of the scattering amplitude [42]. In contrast to the convergence of the three-body energy, the convergence of the asymptotics of the three-body wave function is quite slow and requires many additional three-body channels with large orbital angular momenta. Our results show that the overlap integrals of the three-body and the deuteron wave functions for the cases of $K_{\text{max}} = 20$ and $K_{\text{max}} = 24$ are identical up to the distance of $R = 5.5$ fm, however they behave differently beyond the internal region. The values of the S-wave overlap integral for $K_{\text{max}} = 20$ are 4.2×10^{-3} , 1.2×10^{-5} , 2.5×10^{-8} and $2.2 \times 10^{-13} \text{ fm}^{-1/2}$ at $R=10, 20, 30$ and 40 fm, respectively. For the case of $K_{\text{max}} = 24$ we have estimations of 4.6×10^{-3} , 1.9×10^{-5} , 5.0×10^{-8} and 1.2×10^{-11} , respectively. These numbers should be compared with the correct asymptotics of the overlap integral, i.e. 5.7×10^{-3} , 1.1×10^{-4} , 3.0×10^{-6} and $9.5 \times 10^{-8} \text{ fm}^{-1/2}$ at $R=10, 20, 30$ and 40 fm, respectively. Our further study shows

that even $K_{\text{max}} = 30$ results are far from the correct asymptotics: the corresponding numbers are 5.0×10^{-3} , 3.3×10^{-5} , 1.0×10^{-7} and $2.3 \times 10^{-11} \text{ fm}^{-1/2}$, respectively. As we can see the asymptotics is improved with increasing K_{max} , but very slowly. This analysis demonstrates that in order to have the correct three-body asymptotics, one may have to go as high as $K_{\text{max}}=40$, which would require huge computer resources, especially when calculating the Raynal-Revai coefficients in the developed model. However, there is an alternative way, which we use in our study of the capture process. Namely, K_{max} is fixed at 24 and beyond $R=5.5$ fm the overlap integral for the each three-body channel with $l_y = 0$ and 2 (corresponding to the S- and D-wave α -d relative motion) is replaced by its known asymptotic expression. Then this number is multiplied by the corresponding spin-angular matrix element of the E2-transition operator. The results obtained this way for the astrophysical E2 S-factor will be close to that obtained using the three-body wave function with the correct asymptotic behavior.

The overlap integrals are written as

$$I_L(R) = \langle [\Psi_d \otimes Y_L(\Omega_R)]^{1M} | \Psi_f^{1M+} \rangle, \quad (6)$$

where the integration is done over internal coordinates of the deuteron and the angular part of the variable \mathbf{R} . In the present three-body model, over the interval 5 – 10 fm $I_L(R)$ follows the expected asymptotic behavior $C_{\alpha d}^{(L)} W_{-\eta_b, L+1/2}(2k_b R)/R$, where η_b and k_b are the Sommerfeld parameter and wave number calculated at the separation energy 1.474 MeV of the ${}^6\text{Li}$ bound state into α and d [20]. The values of the S-wave and D-wave asymptotic normalization coefficients (ANC) have been estimated for different values of matching point R_0 . We found that S-wave ANC is maximal (consequently optimal) for the matching point at 5.5 fm: $C_{\alpha d}^{(0)} = 2.116 \text{ fm}^{-1/2}$ and $C_{\alpha d}^{(0)} = 2.051 \text{ fm}^{-1/2}$ for Model A and Model B, respectively. The first number is slightly larger than $C_{\alpha d}^{(0)} \approx 2.05 \text{ fm}^{-1/2}$ [20], obtained with $R_0 = 7.75$ fm and in reasonable agreement with the value $C_{\alpha d}^{(0)} \approx 2.30 \text{ fm}^{-1/2}$ extracted in Ref. [42] from experimental data on $\alpha + d$ scattering. The estimated values of D-wave ANC are less than the corresponding values of the S-wave ANC by two orders of magnitude and vary in the range between 2.160×10^{-2} and $2.175 \times 10^{-2} \text{ fm}^{-1/2}$ for model A for matching points from $R_0 = 5.5$ fm to 7.5 fm. Model B yields the range between 2.179×10^{-2} and $2.188 \times 10^{-2} \text{ fm}^{-1/2}$, respectively.

In Fig. 3 the overlap integrals $I_0(r)$ and $I_2(r)$ with the initial three-body and the asymptotics corrected at $R_0 = 5.5$ fm, within Model A are displayed. The S-wave overlap integral changes the sign at small distances due to orthogonality to the $\alpha - d$ Pauli-forbidden state, this is why the absolute values of the overlap integrals are shown. As can be seen from the figure, beyond about 10 fm the absolute value of $I_L(R)$ decreases faster than the correct asymptotics. Hence, within the three-body model, the E2 astrophysical S-factor is underestimated at

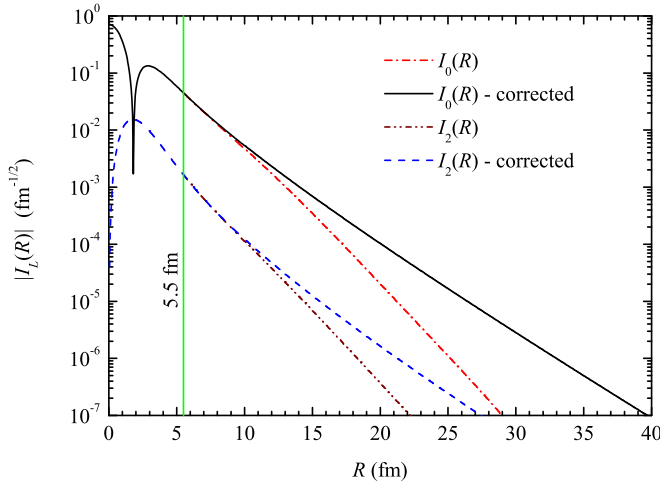


FIG. 3. Overlap integral with the initial three-body and the corrected (at $R_0=5.5$ fm) asymptotics within Model A.

low collision energies. This is the motivation to estimate the E2 S-factor with corrected asymptotics of the overlap integral.

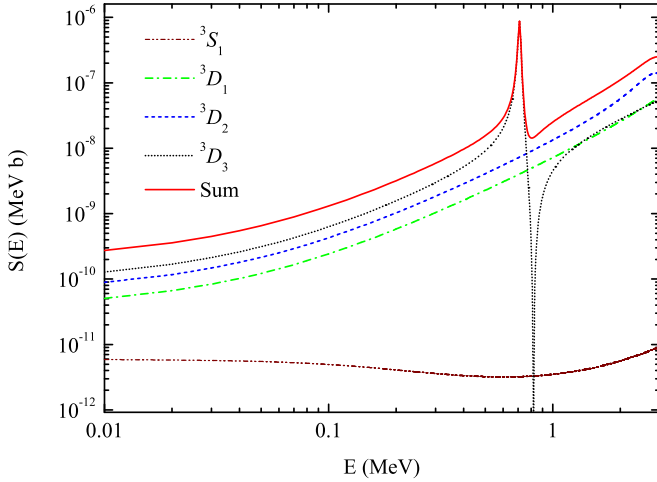


FIG. 4. Partial E2 astrophysical S-factors of the direct $\alpha + d \rightarrow {}^6\text{Li} + \gamma$ capture process within Model A with the corrected asymptotics of the overlap integral.

In Fig. 4 we show E2 astrophysical S-factors for the direct $\alpha + d \rightarrow {}^6\text{Li} + \gamma$ capture process within Model A from the initial 3S_1 , 3D_1 , 3D_2 , 3D_3 partial waves to the ground state of ${}^6\text{Li}$ with the corrected asymptotics of $I_0(R)$ and $I_2(R)$ at a distance $R_0 = 5.5$ fm. As can be seen from the figure, at low energies the contribution of the partial 3S_1 $\alpha + d$ configuration is less than the contributions of partial D-waves at least by an order of magnitude. However, the S-wave contribution has a weak energy dependence, while the smallest 3D_1 wave contribution increases sharply from 5×10^{-11} up to 6×10^{-8} MeV b within the same energy interval.

The influence of the D-wave correction to the asymp-

totics for the E2 S-factor is mostly important at low energies. The results for the E2 S-factor from the initial 3S_1 α -d scattering state increases several times through the correction to the D-wave asymptotics. However, it is still small in comparison with the E2 S-factor from the initial D-wave α -d scattering states. In Model A at energy $E=1$ keV the E2 S-factor for the initial 3S_1 α -d scattering state increases from 1.55×10^{-12} to 5.96×10^{-12} MeV b, while the total E2 S-factor changes slightly from 2.042×10^{-10} to 2.068×10^{-10} MeV b. At the same time, the correction to the S-wave asymptotics sharply enhances the E2 S-factor from 2.537×10^{-11} to 2.042×10^{-10} MeV b due to the initial D-wave α -d scattering states.

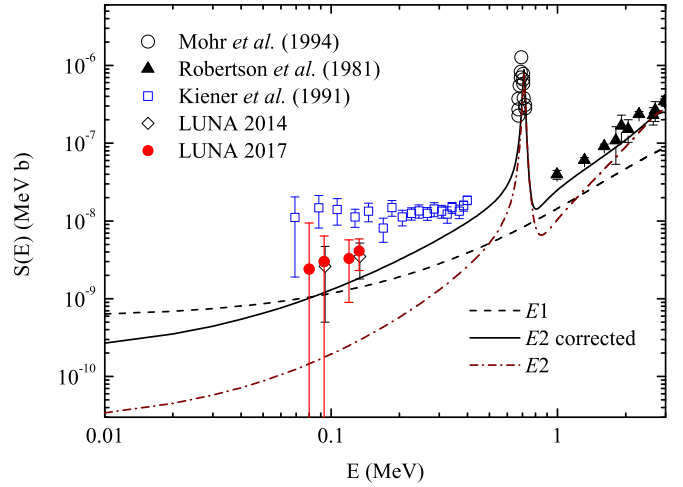


FIG. 5. Relative contributions of the E1 and E2 astrophysical S-factors of the direct $\alpha + d \rightarrow {}^6\text{Li} + \gamma$ capture process within Model A in comparison with available experimental data.

In Fig. 5 we compare the E1 and E2 transition components of the S-factor with available experimental data, including recent data from Refs. [8, 9]. As can be seen from the figure, at low energies the E1 transition dominates even with corrected asymptotics of the overlap integral for the E2 transition, while at higher energies the E2 component is stronger. Finally, in Fig. 6 we compare the obtained theoretical results for the astrophysical S-factor of the direct $\alpha + d \rightarrow {}^6\text{Li} + \gamma$ capture process with experimental data from Refs. [8–10, 51, 52]. One can note that Figs. 5 and 6 are very similar to Figs. 2 and 3 of Ref. [20], respectively. In fact, presently we include also a correction to the D-wave asymptotics of the overlap integral. As discussed above the influence of the D-wave correction to the asymptotics on the S-factor is about 1%

As was noted in Ref. [20], the E2 S-factor can be enhanced owing to the D-wave components of the deuteron, ${}^4\text{He}$ and the final ${}^6\text{Li}$ nucleus with the help of tensor forces in microscopic *ab-initio* models. Together with the aforementioned weak dependence of the E2 S-factor from the initial S-wave at very low energies this can lead to a larger S-wave contribution for the process at low astrophysical energies.

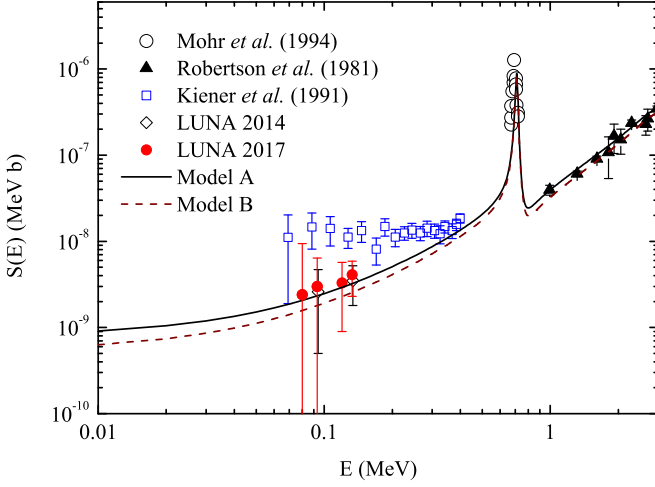


FIG. 6. Theoretical astrophysical S-factor for the direct $\alpha + d \rightarrow {}^6\text{Li} + \gamma$ capture process within Models A and B in comparison with available experimental data.

C. Reaction rates and abundance

In Table I we give theoretical estimations for the $d(\alpha, \gamma){}^6\text{Li}$ reaction rates in the temperature interval $10^6 \text{ K} \leq T \leq 10^{10} \text{ K}$ ($0.001 \leq T_9 \leq 10$) calculated with the two $\alpha + N$ potentials of Voronchev *et al.* [44] (Model A) and Kanada *et al.* [45] (Model B). In the second and third columns of the table we give "the most effective energy" E_0 and the width of the Gamov window ΔE_0 (5). They are expressed as [36]:

$$E_0 = \left(\frac{\mu}{2}\right)^{1/3} \left(\frac{\pi e^2 Z_1 Z_2 k_B T}{\hbar}\right)^{2/3} \\ = 0.122 (Z_1^2 Z_2^2 A)^{1/3} T_9^{2/3} [\text{MeV}], \quad (7)$$

and

$$\Delta E_0 = 4 (E_0 k_B T / 3)^{1/2} \\ = 0.2368 (Z_1^2 Z_2^2 A)^{1/6} T_9^{5/6} [\text{MeV}]. \quad (8)$$

Now we discuss the influence of the D-wave correction of the overlap integral on the reaction rates. The theoretical estimations for the reaction rates increase after the correction to the D-wave asymptotics of the overlap integral by no more than 1% at low temperatures $T_9 \leq 0.1$. In other words, its influence is of the same order as for the E2 S-factor. However, we have shown, that a contribution of the initial 3S_1 α -d scattering state to the E2 S-factor can increase several times after the correction to the D-wave asymptotics of the overlap integral at low energies. This feature is very important for the development of the three-body and microscopic models including tensor forces which give rise to the D-wave components of the final state wave function.

In Fig. 7 we display the estimated reaction rates of the direct $\alpha + d \rightarrow {}^6\text{Li} + \gamma$ capture process within Models

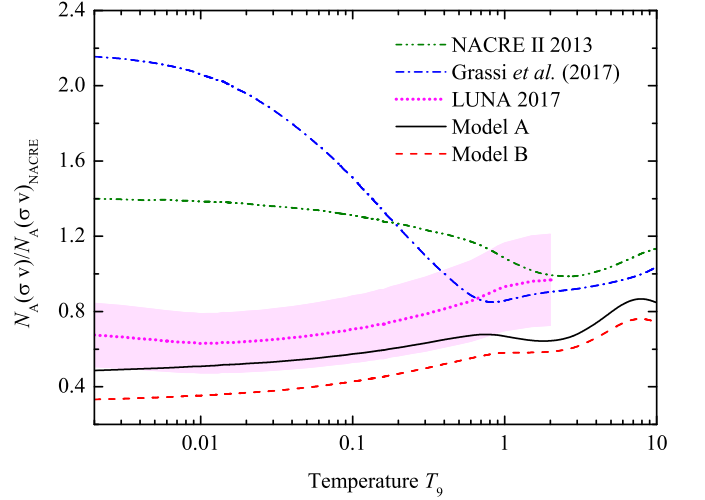


FIG. 7. Reaction rates of the direct $\alpha + d \rightarrow {}^6\text{Li} + \gamma$ capture process within Models A and B normalized to the NACRE 1999 experimental data.

A and B normalized to the standard NACRE 1999 experimental data [53]. For comparison we also display the lines corresponding to the adopted values of the NACRE II 2013 data [54], new LUNA 2017 [55] data and data fit from Ref. [56]. As can be seen from the figure, our results obtained within Models A and B show the same temperature dependence at low values of T_9 , as the newest direct data of the LUNA 2017 [55] and differs from the data NACRE II 2013 [54] and the data fit in Ref. [56]. Consequently, the corresponding energy dependence of the astrophysical S-factor, obtained in the developed theoretical model is mostly consistent with the last direct data of the LUNA collaboration [55].

For the estimation of the primordial abundance of the ${}^6\text{Li}$ element we use the well known PARthENoPE [57] public code, which however operates only with an analytical form of the reaction rate dependence on the temperature T_9 . This way the theoretical reaction rate is approximated within 1.84% (Model A) and 2.46 % (Model B) using the following analytical formula:

$$N_A(\sigma v) = p_0 T_9^{-2/3} \exp(-7.423 T_9^{-1/3}) \\ \times \left[1 + p_1 T_9^{1/3} + p_2 T_9^{2/3} + p_3 T_9 + p_4 T_9^{4/3} \right. \\ \left. + p_5 T_9^{5/3} + p_6 T_9^2 + p_7 T_9^{7/3} \right] \\ + p_8 T_9^{-3/2} \exp(-7.889 T_9^{-1}). \quad (9)$$

The coefficients of the analytical polynomial approximation of the $d(\alpha, \gamma){}^6\text{Li}$ reaction rates estimated with the $\alpha + N$ potential of Voronchev *et al.* (Model A) and Kanada *et al.* (Model B) are given in Table II in the temperature interval ($0.001 \leq T_9 \leq 10$).

On the basis of the theoretical reaction rates and with the help of the PARthENoPE [57] public code we have estimated the primordial abundance of the ${}^6\text{Li}$ element.

TABLE I. Theoretical estimations of the direct $d(\alpha, \gamma)^6\text{Li}$ capture reaction rate in the temperature interval $10^6 \text{ K} \leq T \leq 10^{10} \text{ K}$ ($0.001 \leq T_9 \leq 10$).

T_9	E_0 (MeV)	ΔE_0 (MeV)	$N_A(\sigma v)$ ($\text{cm}^3\text{mol}^{-1}\text{s}^{-1}$)		T_9	E_0 (MeV)	ΔE_0 (MeV)	$N_A(\sigma v)$ ($\text{cm}^3\text{mol}^{-1}\text{s}^{-1}$)	
			Model A	Model B				Model A	Model B
0.001	0.002	0.001	3.47×10^{-30}	2.37×10^{-30}	0.120	0.052	0.054	1.83×10^{-5}	1.38×10^{-5}
0.002	0.003	0.002	1.04×10^{-23}	7.14×10^{-24}	0.130	0.055	0.057	2.68×10^{-5}	2.03×10^{-5}
0.003	0.004	0.003	1.42×10^{-20}	9.74×10^{-21}	0.140	0.058	0.061	3.79×10^{-5}	2.88×10^{-5}
0.004	0.005	0.003	1.33×10^{-18}	9.18×10^{-19}	0.150	0.060	0.064	5.21×10^{-5}	3.96×10^{-5}
0.005	0.006	0.004	3.36×10^{-17}	2.32×10^{-17}	0.160	0.063	0.068	6.96×10^{-5}	5.31×10^{-5}
0.006	0.007	0.004	3.93×10^{-16}	2.72×10^{-16}	0.180	0.068	0.075	1.17×10^{-4}	8.96×10^{-5}
0.007	0.008	0.005	2.79×10^{-15}	1.93×10^{-15}	0.200	0.073	0.082	1.83×10^{-4}	1.41×10^{-4}
0.008	0.009	0.006	1.41×10^{-14}	9.77×10^{-15}	0.250	0.085	0.099	4.53×10^{-4}	3.54×10^{-4}
0.009	0.009	0.006	5.52×10^{-14}	3.83×10^{-14}	0.300	0.096	0.115	9.17×10^{-4}	7.23×10^{-4}
0.010	0.010	0.007	1.79×10^{-13}	1.25×10^{-13}	0.350	0.106	0.131	1.62×10^{-3}	1.29×10^{-3}
0.011	0.011	0.007	5.00×10^{-13}	3.48×10^{-13}	0.400	0.116	0.146	2.62×10^{-3}	2.10×10^{-3}
0.012	0.011	0.008	1.24×10^{-12}	8.66×10^{-13}	0.500	0.134	0.176	5.68×10^{-3}	4.60×10^{-3}
0.013	0.012	0.008	2.80×10^{-12}	1.96×10^{-12}	0.600	0.152	0.205	1.06×10^{-2}	8.67×10^{-3}
0.014	0.012	0.009	5.82×10^{-12}	4.08×10^{-12}	0.700	0.168	0.233	1.79×10^{-2}	1.49×10^{-2}
0.015	0.013	0.010	1.13×10^{-11}	7.94×10^{-12}	0.800	0.184	0.260	2.88×10^{-2}	2.43×10^{-2}
0.016	0.014	0.010	2.08×10^{-11}	1.46×10^{-11}	0.900	0.199	0.287	4.43×10^{-2}	3.80×10^{-2}
0.018	0.015	0.011	6.11×10^{-11}	4.30×10^{-11}	1.000	0.213	0.313	6.56×10^{-2}	5.70×10^{-2}
0.020	0.016	0.012	1.55×10^{-10}	1.09×10^{-10}	1.500	0.279	0.439	2.72×10^{-1}	2.45×10^{-1}
0.025	0.018	0.015	9.90×10^{-10}	7.03×10^{-10}	2.000	0.338	0.558	6.04×10^{-1}	5.50×10^{-1}
0.030	0.021	0.017	4.08×10^{-9}	2.91×10^{-9}	2.500	0.393	0.672	9.88×10^{-1}	8.99×10^{-1}
0.040	0.025	0.021	3.23×10^{-8}	2.32×10^{-8}	3.000	0.443	0.782	1.39	1.26
0.050	0.029	0.026	1.41×10^{-7}	1.02×10^{-7}	4.000	0.537	0.994	2.26	2.02
0.060	0.033	0.030	4.35×10^{-7}	3.18×10^{-7}	5.000	0.623	1.197	3.24	2.87
0.070	0.036	0.034	1.07×10^{-6}	7.88×10^{-7}	6.000	0.704	1.393	4.35	3.83
0.080	0.040	0.038	2.26×10^{-6}	1.67×10^{-6}	7.000	0.780	1.584	5.54	4.87
0.090	0.043	0.042	4.27×10^{-6}	3.17×10^{-6}	8.000	0.853	1.771	6.78	5.95
0.100	0.046	0.046	7.38×10^{-6}	5.51×10^{-6}	9.000	0.922	1.953	8.05	7.06
0.110	0.049	0.050	1.19×10^{-5}	8.94×10^{-6}	10.00	0.989	2.133	9.31	8.16

TABLE II. The fitting coefficients of the analytical approximation for the direct $d(\alpha, \gamma)^6\text{Li}$ capture reaction rate.

Model	p_0	p_1	p_2	p_3	p_4	p_5	p_6	p_7	p_8
A	6.004	-2.558	34.730	-115.482	205.801	-169.456	71.428	-11.614	42.354
B	5.154	-5.830	52.356	-163.500	272.839	-218.444	89.174	-14.107	41.384

If we adopt the Planck 2015 best fit for the baryon density parameter $\Omega_b h^2 = 0.02229^{+0.00029}_{-0.00027}$ [58] and the neutron life time $\tau_n = 880.3 \pm 1.1 \text{ s}$ [59], for the $^6\text{Li}/\text{H}$ abundance ratio we have an estimation from 0.66×10^{-14} to 0.68×10^{-14} within Model A. Model B yields an estimation from 0.49×10^{-14} to 0.51×10^{-14} . The results of Model A are mostly consistent with the new estimation $^6\text{Li}/\text{H} = (0.80 \pm 0.18) \times 10^{-14}$ of the LUNA collaboration [55] than the models based on the exact mass prescription method [56]

$^6\text{Li}/\text{H} = (0.90 - 1.8) \times 10^{-14}$. Finally, using this result and the estimate of the $^7\text{Li}/\text{H}$ abundance ratio of $(5.2 \pm 0.4) \times 10^{-10}$ from Ref. [60] we get $^6\text{Li}/^7\text{Li} = (1.30 \pm 0.12) \times 10^{-5}$ which agrees with the standard estimate from the BBN model [3].

As noted before the OPP method [46] has been used for the treatment of Pauli forbidden states in the three-body system resulting from the S-wave $\alpha - N$ deep interaction potential. In addition, an alternative method for elim-

inating the three-body Pauli forbidden states based on the SUSY method [47] has been tested. The results indicated that the SUSY method yields too small isotriplet ($T = 1$) component of the ${}^6\text{Li}$ ground state which play the main role in the description of E1 S-factor, although the energy value of the ground state was reproduced at the same level as in the case of the OPP method. Indeed, the norm square of the isotriplet component was estimated to be 1.102×10^{-4} and 1.104×10^{-4} within Models A and B, respectively. These numbers are about 50 and 40 times less than the corresponding estimations obtained within the OPP method. A similar level of decreasing was observed for the corresponding E1 S-factor, although the E2 S-factor was very close to the one resulting from the OPP method. Most likely, the SUSY method suppresses important isotriplet components of the ${}^6\text{Li}$ ground state wave function. These results indicate that the isospin forbidden E1-transition depends strongly on the method used for elimination of Pauli forbidden states in many body systems.

IV. CONCLUSIONS

The astrophysical direct capture process $\alpha + d \rightarrow {}^6\text{Li} + \gamma$ has been studied in the three-body model. The reaction rates, E1 and E2 astrophysical S-factors as well as the primordial abundance of the ${}^6\text{Li}$ element have been estimated. The asymptotics of the overlap integral in the S- and D-waves have been corrected. This increased the E2 S-factor by an order of magnitude at low astrophysical energies mostly due to the S-wave corrections. The D-wave correction yields only about 1% increase to the

total S-factor and the reaction rates at low energies. Together with the corrected E2 S-factor, the contribution of the E1-transition operator to the S-factor from the initial isosinglet states to the small isotriplet components of the final ${}^6\text{Li}(1+)$ bound state is shown to be able to reproduce the new experimental data of the LUNA collaboration within the experimental error bars. The theoretical reaction rates have the same temperature dependence at low temperatures as the newest direct 2017 data of the LUNA collaboration. For the abundance ratio ${}^6\text{Li}/\text{H}$ we have obtained an estimation $(0.67 \pm 0.01) \times 10^{-14}$, consistent with the new estimation of the LUNA collaboration and much lower than the results of the models based on the exact mass prescription. Further improvement of the theoretical estimations of the reaction rates and ${}^6\text{Li}$ abundance is expected with the help of NN-tensor forces within *ab-initio* calculations. It is established that the isospin forbidden E1-transition is highly sensitive to the method used for treating the Pauli forbidden states in three-body systems.

ACKNOWLEDGMENTS

The authors acknowledge Daniel Baye and Pierre Descouvemont for useful discussions and valuable advice. E.M.T. acknowledges a visiting scholarship from the Curtin Institute for Computation and thanks members of the Theoretical physics group at Curtin University for the kind hospitality during his visit. The support of the Australian Research Council, the Australian National Computer Infrastructure, and the Pawsey Supercomputer Centre are gratefully acknowledged.

-
- [1] L. Sbordone, P. Bonifacio, E. Caffau et al., *Astron. Astrophys.* **522**, A26 (2010).
 - [2] A. M. Mukhamedzhanov, Shubhchintak, and C. A. Bertulani, *Phys. Rev. C* **93**, 045805 (2016).
 - [3] P. D. Serpico, S. Esposito, F. Iocco, G. Mangano, G. Miele, and O. Pisanti, *J. Cosmol. Astropart. Phys.* **2004**, 010 (2004).
 - [4] M. Asplund, D. L. Lambert, P. E. Nissen, F. Primas, and V. V. Smith, *Astrophys. J.* **644**, 229 (2006).
 - [5] T. Neff, *Phys. Rev. Lett.* **106** 042502 (2011).
 - [6] J. Dohet-Eraly, P. Navratil, S. Quaglioni, W. Horiuchi, G. Hupin, and F. Raimondi, *Phys. Lett. B* **757** 430 (2016).
 - [7] E. M. Tursunov, S. A. Turakulov, A. S. Kadyrov, *Phys. Rev. C* **97** 035802 (2018).
 - [8] M. Anders, D. Trezzi, R. Menegazzo, M. Aliotta, A. Bellini, D. Bemmerer, C. Broggini, A. Cacioli, P. Corvisiero, H. Costantini, T. Davinson, Z. Elekes, M. Erhard, A. Formicola, Z. Fülöp, G. Gervino, A. Guglielmetti, C. Gustavino, G. Gyürky, M. Junker, A. Lemut, M. Marta, C. Mazzocchi, P. Prati, C. Rossi Alvarez, D. A. Scott, E. Somorjai, O. Straniero, and T. Szücs (LUNA Collaboration), *Phys. Rev. Lett.* **113**, 042501 (2014).
 - [9] D. Trezzi, M. Anders, M. Aliotta *et al.* *Astropart. Phys.* **89** 57 (2017).
 - [10] J. Kiener, H. J. Gils, H. Rebel, S. Zagromski, G. Gsottschneider, N. Heide, H. Jelitto, J. Wentz, and G. Baur, *Phys. Rev. C* **44**, 2195 (1991).
 - [11] S. B. Dubovichenko and A. V. Dzhezairov-Kakhramanov, *Phys. At. Nucl.* **58**, 579 (1995).
 - [12] S. B. Dubovichenko and A. V. Dzhezairov-Kakhramanov, *Phys. At. Nucl.* **58**, 788 (1995).
 - [13] S. Typel, H. Wolter, and G. Baur, *Nucl. Phys. A* **613**, 147 (1997).
 - [14] A. M. Mukhamedzhanov, L. D. Blokhintsev, and B. F. Irgaziev, *Phys. Rev. C* **83**, 055805 (2011).
 - [15] E. M. Tursunov, S. A. Turakulov, and P. Descouvemont, *Phys. At. Nucl.* **78**, 193 (2015).
 - [16] K. M. Nollett, R. B. Wiringa, and R. Schiavilla, *Phys. Rev. C* **63**, 024003 (2001).
 - [17] S. Typel, G. Blüge, and K. Langanke, *Z. Phys. A* **339** 335 (1991).
 - [18] A. Kharbach and P. Descouvemont, *Phys. Rev. C* **58**, 1066 (1998).
 - [19] K. Langanke, *Nucl. Phys. A* **457**, 351 (1986).

- [20] D. Baye and E. M. Tursunov, J. Phys. G: Nucl. Part. Phys. **45** 085102 (2018).
- [21] Shubhchintak, C A Bertulani, A M Mukhamedzhanov and A T Kruppa, J. Phys. G: Nucl. Part. Phys. **43** 125203 (2016).
- [22] E. M. Tursunov, A. S. Kadyrov, S. A. Turakulov and I. Bray, Phys. Rev. C **94** 015801 (2016).
- [23] P. Descouvemont, C. Daniel, and D. Baye, Phys. Rev. C **67**, 044309 (2003).
- [24] E. M. Tursunov, D. Baye, and P. Descouvemont, Phys. Rev. C **73**, 014303 (2006).
- [25] M. V. Zhukov, B. V. Danilin, D. V. Fedorov, J. M. Bang, I. J. Thompson and J. S. Vaagen, Phys. Rep. **231** 151 (1993)
- [26] I. J. Thompson, B. V. Danilin, V. D. Efros, J. S. Vaagen, J. M. Bang, and M. V. Zhukov Phys. Rev. **C61**, 024318 (2000)
- [27] P. Descouvemont, E. Tursunov, and D. Baye, Nucl. Phys. **A765** 370 (2006)
- [28] I.J. Thompson, F.M. Nunes, and B.V. Danilin, Comp. Phys. Comm. **161** 87 (2004)
- [29] N. B. Nguyen, F. M. Nunes, I. J. Thompson, and E. F. Brown, Phys. Rev. Lett. **109** 141101 (2012)
- [30] M. Rodriguez-Gallardo, J. M. Arias, J. Gmez-Camacho, A. M. Moro, I. J. Thompson, and J. A. Tostevin, Phys. Rev. C **72**, 024007 (2005)
- [31] J. Casal, M. Rodriguez-Gallardo and J. M. Arias, Phys. Rev. C **88** 014327 (2013)
- [32] A. E. Lovell, F. M. Nunes and I. J. Thompson, Phys. Rev. **C95** 034605 (2017)
- [33] P. Descouvemont, T. Druet, L. F. Canto and M. S. Hussein, Phys. Rev. C **91** 024606 (2015)
- [34] T. Matsumoto, T. Kamizato, K. Ogata, Y. Iseri, E. Hiyama, M. Kamimura, and M. Yahiro, Phys. Rev. C **68** 064607 (2003)
- [35] R. de Diego, E. Garrido, D.V. Fedorov and A. S. Jensen, Eur.Phys. Lett. **90** 52001 (2010)
- [36] C. Angulo, M. Arnould, M. Rayet, P. Descouvemont, D. Baye, C. Leclercq-Willain, A. Coc, S. Barhoumi, P. Aguer, C. Rolfs, R. Kunz, J. Hammer, A. Mayer, T. Paradellis, S. Kossionides, C. Chronidou, K. Spyrou, S. Degl'Innocenti, G. Fiorentini, B. Ricci, S. Zavatarelli, C. Providencia, H. Wolters, J. Soares, C. Grama, J. Rahighi, A. Shotter, and M. L. Racht, Nucl. Phys. A **656**, 3 (1999).
- [37] W. A. Fowler, G. R. Caughlan, and B. A. Zimmerman, Annu. Rev. Astron. Astrophys. **13**, 69 (1975) .
- [38] D. Thompson, M. Lemere, and Y. Tang, Nucl. Phys. A **286**, 53 (1977) .
- [39] I. Reichstein and Y. C. Tang, Nucl. Phys. A **158** 529 (1970).
- [40] D. Baye, Phys. Rep. **565**, 1 (2015).
- [41] S. B. Dubovichenko and A. V. Dzhezairov-Kakhramanov, Phys. At. Nucl. **57**, 733 (1994).
- [42] L. D. Blokhintsev, V. I. Kukulin, A. A. Sakharuk, D. A. Savin, and E. V. Kuznetsova, Phys. Rev. C **48**, 2390 (1993).
- [43] E. M. Tursunov, P. Descouvemont and D. Baye, Nucl. Phys. A **793** 52 (2007).
- [44] V. Voronchev, V. Kukulin, V. Pomerantsev, and G. Ryzhikh, Few-Body Syst. **18**, 191 (1995).
- [45] H. Kanada, T. Kaneko, S. Nagata and M. Nomoto, Prog. Theor. Phys. **61** 1327 (1979).
- [46] V. I. Kukulin, V. N. Pomerantsev, A. Faessler, A. Buchmann, and E.M. Tursunov, Phys.Rev. **C57** 535 (1998)
- [47] D. Baye, Phys. Rev. Lett. **58** 2738 (1987)
- [48] I. Tanihata, T. Kobayashi, O. Yamakawa, S. Shimoura, K. Ekuni, K. Sugimoto, N. Takahashi, T. Shimoda, and H. Sato, Phys. Lett. B **206**, 592 (1988).
- [49] L. D. Blokhintsev, A. S. Kadyrov, A. M. Mukhamedzhanov, and D. A. Savin, Phys. Rev. C **95**, 044618 (2017).
- [50] L. D. Blokhintsev, A. S. Kadyrov, A. M. Mukhamedzhanov, and D. A. Savin, Phys. Rev. C **97**, 024602 (2018).
- [51] P. Mohr, V. Kölle, S. Wilmes, U. Atzrott, G. Staudt, J. W. Hammer, H. Krauss, and H. Oberhummer, Phys. Rev. C **50**, 1543 (1994).
- [52] R. G. H. Robertson, P. Dyer, R. A. Warner, R. C. Melin, T. J. Bowles, A. B. McDonald, G. C. Ball, W. G. Davies, and E. D. Earle, Phys. Rev. Lett. **47**, 1867 (1981).
- [53] C. Angulo *et al.* (NACRE), Nucl. Phys. A **656** 3 (1999).
- [54] Y. Xu, K. Takahashi, S. Gorielya, M. Arnould, M. Ohtac, H. Utsunomiya (NACRE II). Nucl. Phys. A **918** 61 (2013).
- [55] D. Trezzi, M. Anders, M. Aliotta *et al.* (LUNA collaboration), Astropart. Phys. **89** 57 (2017).
- [56] A. Grassi, G. Mangano, L.E. Marcucci and O. Pisanti, Phys. Rev. C **96** 045807 (2017).
- [57] O. Pisanti, A. Cirillo, S. Esposito, F. Iocco, G. Mangano, G. Miele, and P. D. Serpico, Comput. Phys. Commun. **178** 956 (2008).
- [58] P. A. R. Ade *et al.* (Planck Collaboration), Astron. Astrophys. **594** A13 (2016).
- [59] K. A. Olive, K. Agashe, C. Amsler *et al.*, Chin. Phys. C, **38** 090001 (2014).
- [60] A. Kontos, E. Uberseder, R. deBoer, J. Görres, C. Akers, A. Best, M. Couder, M. Wiescher, Phys. Rev. C **87** (2013) 065804 (2013).